



Adaptive emission profile of transformable fluorescent probes as fingerprints: A typical application in distinguishing different surfactants

Guangying Wang^{a,b,c}, Qinglong Qiao^{b,*}, Wenhao Jia^b, Yiyan Ruan^b, Kai An^b,
Wenchao Jiang^b, Xuelian Zhou^{a,b}, Zhaochao Xu^{a,b,*}

^a School of Chemistry, Dalian University of Technology, Dalian 116024, China

^b Dalian Institute of Chemical Physics, Chinese Academy of Sciences, Dalian 116023, China

^c University of Chinese Academy of Sciences, Beijing 100049, China

ARTICLE INFO

Article history:

Received 17 May 2024

Revised 13 June 2024

Accepted 14 June 2024

Available online 14 June 2024

Keywords:

Sensor

AEPF

Probe

Aggregates

Surfactants

Distinguish

ABSTRACT

The overuse of surfactants has made them well-known environmental pollutants. So far, it is still a challenge to simultaneously distinguish cationic, anionic, zwitterionic, nonionic surfactants and surfactants with similar structures based on traditional analytical techniques. We developed a high-throughput method for distinguishing various surfactants based on the adaptive emission profile as fingerprints (AEPF). The fluorescence response of the sensor was based on the interaction between surfactants and 1,3-diacetylpyrene (**o-DAP**) probe. The interaction affected the reversible conversion of free molecules and two aggregates in the solution, thereby changing the relative abundance and the fluorescence intensity ratio of two aggregates emitting different fluorescence. The **o-DAP** sensor can distinguish four types of surfactants (16 surfactants), especially surfactants of the same type with similar structures. The **o-DAP** sensor sensitively determined the critical micelle concentration (CMC) of 16 surfactants based on the interaction between **o-DAP** and surfactants. Additionally, the **o-DAP** sensor can detect and distinguish artificial vesicles made from different surfactants.

© 2025 Published by Elsevier B.V. on behalf of Chinese Chemical Society and Institute of Materia Medica, Chinese Academy of Medical Sciences.

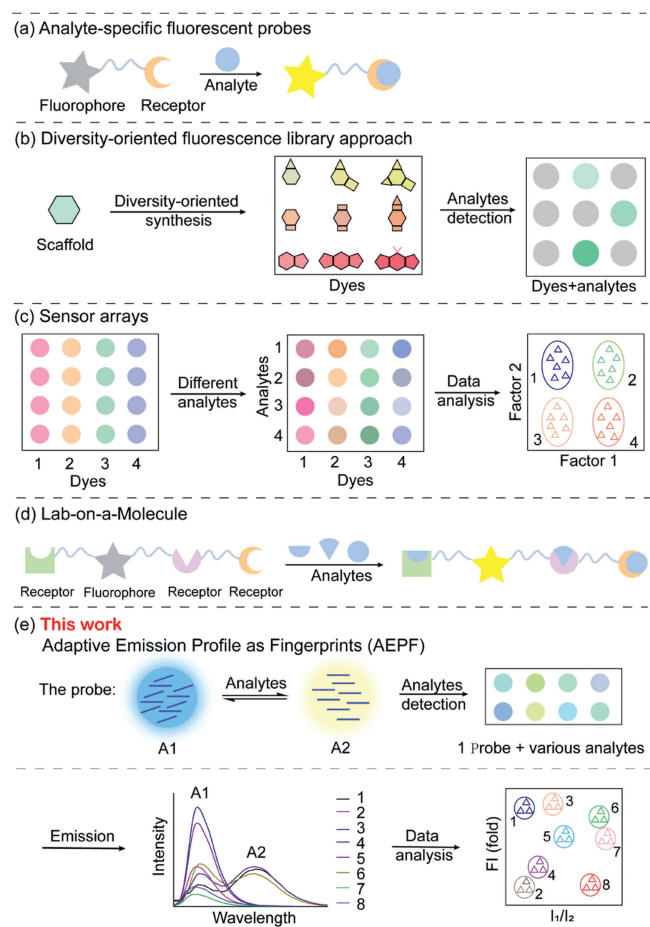
Surfactants, amphiphilic organic molecules composed of one or more hydrophobic tails linked to a hydrophilic head, can significantly reduce the surface tension of solutions, making them widely used as household detergents, personal cleansers, disinfectants [1]. They are classified according to the charge of hydrophilic group into cationic, anionic, zwitterionic, and nonionic surfactants [2]. This differentiation enables them to serve unique functions tailored to specific applications and conditions. For example, surfactant-based products for contraception have been used for decades [3]. Approximately 230,000 tons of surfactants were used in agrochemicals every year, serving as plasticizers to enhance the mobility of agrochemicals on crops [4]. However, the excessive use of surfactants results in the generation of significant amounts of surfactant-containing wastewater and waste residues. These byproducts are frequently discharged into water bodies, soil, and other environments, exacerbating environmental pollution and posing health risks [5,6]. Prolonged exposure to relatively high concentrations of

surfactants may cause skin abrasion, as surfactants disrupt the lipid layer of the cells [7]. Anionic surfactants in surface waters significantly inhibited the growth of invertebrates and fish due to electrostatic interactions between surfactants and proteins [8-10]. Nonionic surfactants inhibited antioxidant enzymes and caused oxidative stress in zebrafish embryos [11]. In addition to these biological hazards, some surfactants were illegally used as masking agents by a few athletes to interfere with the identification of illegal drugs in doping tests [12]. Therefore, identifying the four types of surfactants, as well as surfactants with similar structures, appears great urgent.

Fluorescent sensors play a pivotal role in the field of analytical sensors due to their high sensitivity, simple operation, and rapid response time. Traditional fluorescence sensors consist of three parts: A fluorophore, a linker, and a receptor. The fluorescence response occurs through specific binding of the target analyte (Scheme 1a) [13-16]. The sensors can only identify a target analyte, which hinders its application in distinguishing multiple analytes such as surfactants [17-20]. To circumvent the limitations of specific recognition probes, chemists have developed diversity-oriented fluorescence library approaches (Scheme 1b). Diversity-

* Corresponding authors.

E-mail addresses: qqjqiao@dicp.ac.cn (Q. Qiao), zcxu@dicp.ac.cn (Z. Xu).



Scheme 1. Schematic diagram of fluorescent sensors. (a) The "lock-and-key" methodology. (b) The diversity-oriented fluorescence library approaches. (c) The fluorescent array sensors. (d) Lab on a molecule. (e) AEPF. A1 and A2 represented the aggregates with fluorescence peaks at shorter wavelengths and longer wavelengths, respectively.

oriented synthesis (DOS) is from the derivatization of fluorophore scaffolds, where diverse groups are introduced into the fluorophore scaffold to synthesize a multi-purpose fluorescent probe library. Multiple analytes are tested in a high-throughput manner, screening these fluorescent probe libraries to generate a potential sensor library [21]. While diversity-oriented fluorescence library has significantly accelerated the identification of multiple analytes, this strategy is cumbersome, akin to "finding a needle in a haystack" when faced with multiple analytes such as surfactants. Therefore, researchers rarely employed "lock-and-key" methods and diversity-oriented fluorescence library approaches to identify multiple surfactants.

Inspired by the olfactory or gustatory systems to distinguish multiple analytes such as surfactants, fluorescent sensor arrays have been developed (Scheme 1c) [22]. The sensor arrays has multiple signal channels, with probes in each channel detecting a single signal of the analyte. By simultaneously analyzing multiple signals of the analyte, the sensor arrays generate a specific "fingerprint" for the analyte. The fluorescent sensor array can recognize and distinguish a range of analogues [23]. In recent years, fluorescent sensor arrays have been widely applied to distinguish multiple surfactants. The sensor array based on luminescent metal-organic frameworks (LMOFs, $\text{NH}_2\text{-UiO-66}$ and $\text{NH}_2\text{-MIL-88}$) distinguished five anionic sulfonate surfactants with similar structure [24]. Similarly, the sensor array of $\text{UiO-66-NH}_2\text{@Au NCs}$ specifically distinguished six surfactants [25]. Compared with fluorescent sen-

sor arrays which operate on multi-channel detection with multi-probe, Lab-on-a-molecule probes operate on multi-channel detection with one probe. Lab-on-a-molecule probes are also highly sought after distinguishing multiple similar analytes [26]. Lab-on-a-molecule probe was firstly proposed by A. Prasanna de Silva for rapid screening of medical diseases (Scheme 1d). In recent years, Lab-on-a-molecule probes have been used to distinguish surfactants. NAAN-3 served as a Lab-on-a-molecule and distinguished sodium dodecyl sulfate (SDS) from sodium dodecyl benzene sulfonate (SDBS) [27]. Dual-emission samarium macrocycle served as a Lab-on-a-molecule enabling high-throughput identification of anionic sulfonate surfactants [28]. Although fluorescent array sensors and Lab-on-a-molecule methods were widely used to distinguish various surfactants, it has not been possible to distinguish four surfactants, especially similar surfactants. In a word, it has proven to be a difficult challenge to simply and quickly identify cationic, anionic, zwitterionic, and nonionic surfactants, especially the same type of surfactants with similar structures.

Here, we developed a novel fluorescence sensor based on the adaptive emission profile as fingerprints (AEPF) (Scheme 1e). In 1,3-diacetylpyrene (***o*-DAP**) aqueous solution, there were two aggregates (A1, A2) with different molecular packing, emitting two kinds of fluorescence, which can undergo reversible transformation under environmental influence. The interaction between analytes and ***o*-DAP** affected the reversible conversion of free molecules and two aggregates in the solution, thereby altering the relative abundance and their fluorescence intensity ratio of the two aggregates emitting different fluorescence. After data analysis, each analyte corresponded to a specific "fingerprint". The "fingerprints" of different analytes enabled precise classification. In this work, the sensor sensitively distinguished 16 kinds of surfactants, including cationic, anionic, zwitterionic, and nonionic surfactants, especially the same type of surfactants with similar structures. The feasibility of the AEPF sensor was also demonstrated by sensitive detection of the critical micelle concentration (CMC) of 16 surfactants. Additionally, the sensor can distinguish artificial vesicles made from various surfactants.

The structure of the ***o*-DAP** fluorescent probe was shown in Fig. 1a, and the synthesis step was illustrated in Fig. S1 (Supporting information). ***o*-DAP** exhibited almost no fluorescence in solution, but it emitted strong fluorescence when aggregated, possibly due to the restricted rotation of acetyl group. ***o*-DAP** formed two types of aggregates, A1 and A2, with different molecular arrangements in aqueous solution. The reason was that the arrangement of molecules can affect their luminescence properties [29]. Notably, ***o*-DAP** has a large planar aromatic ring and exhibits strong $\pi\cdots\pi$ and $\text{C-H}\cdots\pi$ interactions, making it particularly sensitive to environmental influences [29]. The fluorescence response of the ***o*-DAP** sensor was attributed to the reversible conversion of free molecules and two luminescent aggregates in the solution (Fig. 1a). Various surfactants with different charges and groups had different interactions with ***o*-DAP**, which lead to varying degrees of decomposition for the two luminescent aggregates and different fluorescence responses. After data analysis, each surfactant corresponded to a specific "fingerprint". The "fingerprints" of various surfactants enabled precise classification (Fig. 1a).

***o*-DAP** exhibited aggregation-induced emission properties, with weak fluorescence in tetrahydrofuran solution (0% H_2O). As the water content increased from 0% to 100%, the color of the solution gradually changed from blue to yellow under ultraviolet (UV) light (Fig. 1b). During this period, aggregates emitting peaks at 445 nm are formed first, followed by the formation of aggregates emitting peaks at 560 nm (Fig. 1c). The interaction between surfactants charges and ***o*-DAP** affected the conversion of two aggregates in the solution. To assess the ability of the ***o*-DAP** sensor to distinguish surfactants, we selected 16 surfactants, comprising four

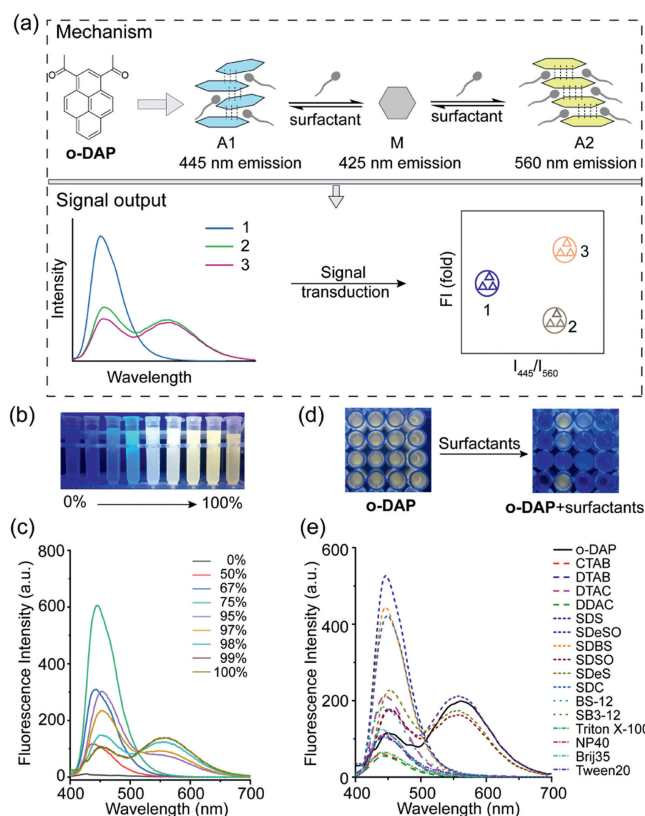


Fig. 1. (a) Schematic of the mechanism and signal output for detecting various surfactants using the **o-DAP** sensor, M represented the free monomer molecules in the solution, while A1 and A2 represented the aggregates with fluorescence peaks at 445 nm and 560 nm, respectively; Fluorescence photographs (b) and fluorescence spectra (c) of **o-DAP** in different volumes of water (water and tetrahydrofuran); Fluorescence photographs (d) and fluorescence spectra (e) of **o-DAP** in various surfactant solutions in PBS (20 mmol/L, pH 7.4). [**o-DAP**] = 10 $\mu\text{mol/L}$; [surfactants] = 20 mmol/L.

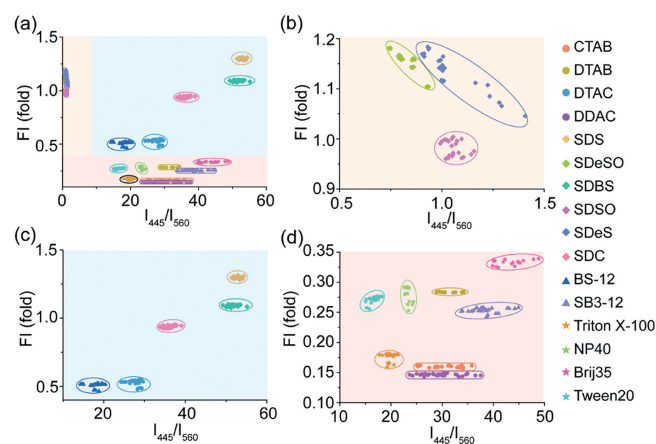


Fig. 2. (a) Fingerprint map of the fluorescence ratio I_{445}/I_{560} and the intensity increment for discriminating cationic, anionic, zwitterionic, nonionic surfactants, and structurally similar surfactants with **o-DAP**. I_{445} and I_{560} represented the fluorescence intensity at 445 nm and 560 nm in the **o-DAP** solution with surfactants, respectively. FI (fold) was the fold increase in the integrated fluorescence intensity of the **o-DAP** solution with surfactants compared to the integrated fluorescence intensity of the **o-DAP** solution. (b–d) Partial enlargements of (a).

types and the similar structure of surfactants: cationic surfactants, including hexadecyl trimethyl ammonium bromide (CTAB), dodecyl trimethyl ammonium bromide (DTAB), dodecyl trimethyl ammonium chloride (DTAC), and didecyl dimethyl ammonium chloride (DDAC); anionic surfactants, such as SDS, sodium decane-1-sulfonate (SDeSO), SDBS, sodium 1-dodecanesulfonate (SDSO), sodium 1-decanesulfonate (SDeS), and sodium deoxycholate (SDC); zwitterionic surfactants, including dodecyl dimethyl betaine (BS-12) and lauryl sulfobetaine (SB3-12); and nonionic surfactants, Triton X-100, substitute octylphenoxy-polyethoxyethanol (NP40), polyoxyethylene lauryl ether (Brij35), and Tween20 (Fig. S2 in Sup-

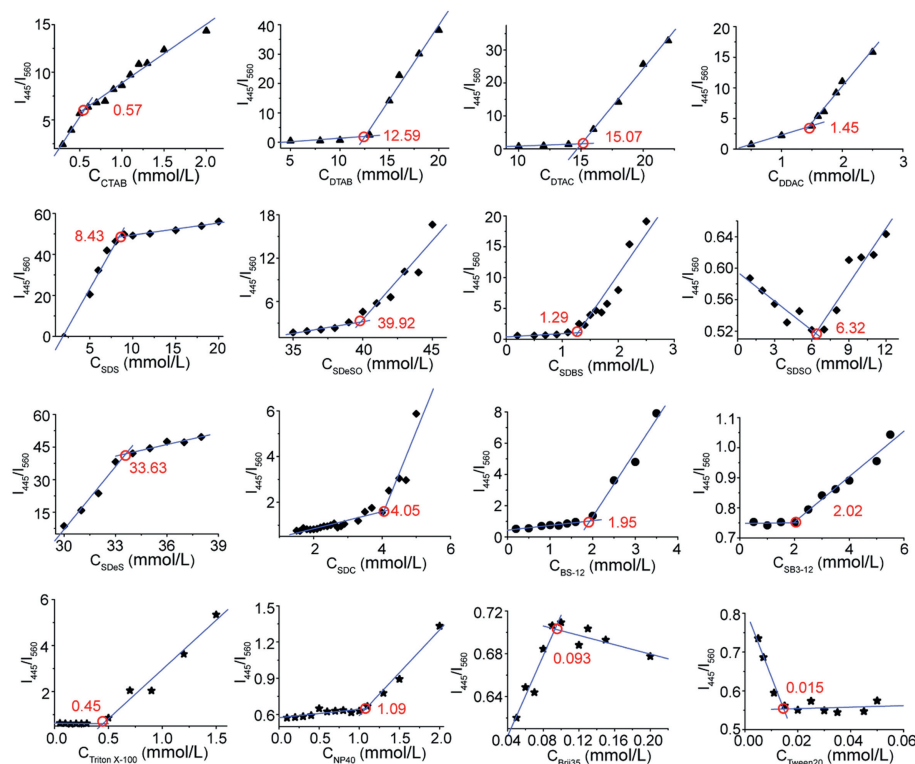


Fig. 3. The fluorescence ratio I_{445}/I_{560} as functions of surfactant concentration to determine the CMC values of CTAB, DTAB, DTAC, DDAC, SDS, SDeSO, SDBS, SDSO, SDeS, SDC, BS-12, SB3-12, Triton X-100, NP40, Brij35, Tween20.

porting information). It was observed that the **o-DAP** solution emitted different fluorescence after adding various surfactants (Fig. 1d, Fig. S3 in Supporting information). The fluorescence spectra of **o-DAP** and 16 surfactants clearly showed the differences in interaction (Fig. 1e).

The combination of the fluorescence intensity ratio I_{445}/I_{560} and the fold increase in fluorescence served as a fingerprint for each surfactant. The **o-DAP** sensor's response to each surfactant underwent parallel experiments for over 15 times, ensuring the accuracy and feasibility of the results. The two-dimensional fingerprint maps of the 16 surfactants were shown in Fig. 2. It was observed that the fingerprints of the 16 surfactants were well-separated and no repetition. This indicated that the **o-DAP** sensor, based on the AEPF, has achieved high-throughput discrimination of cationic, anionic, zwitterionic, and nonionic surfactants, especially those with similar structures in the same type. Compared with traditional fluorescence sensors, **o-DAP** sensors can identify a wider variety of analytes as well as analytes with subtle structural differences.

The CMC is an essential parameter of surfactants, and the lowest concentration required for the formation of micelles in a solvent. The properties of the solution undergo a significant change at this concentration [30]. It has been demonstrated that fluorescence sensors can be used to determine CMC values of surfactants [31]. To further evaluate the ability of the **o-DAP** sensor to respond to various surfactants, fluorescence titration experiments were conducted with different concentrations of the 16 surfactants. In the fluorescence titration experiments, fluorescence spectra varied with different concentrations (Figs. S4–S19 in Supporting information). The I_{445}/I_{560} as functions of concentrations was determined the CMC values of surfactants (Fig. 3, Figs. S20–S35 in Supporting information). It was observed that as the surfactant concentrations increased, there was a distinct transition at the CMC value with different linear behaviors before and after the transition. The CMC value of a surfactant was the intersection point of two straight lines. As shown in Table 1 [2,32–41], the measured CMC values of the surfactants were in excellent agreement with those reported in the literature. Therefore, the **o-DAP** sensor based on AEPF distinguished four types of surfactants, including those with similar structures within the same type.

The **o-DAP** sensor based on AEPF not only sensitively detected four types of surfactants but also identified artificial vesicles made from various surfactants (Fig. 4a). Artificial vesicles made of oil-in-water had their hydrophobic end-groups enclosed within the vesicle, while the hydrophilic end-groups with various charges were neatly arranged on the vesicle surface. The average ratio values of vesicles made from BS-12, DTAC, SDeSO, SDS, SDeSO and SDeS surfactant varied, which was attributed to the different interactions

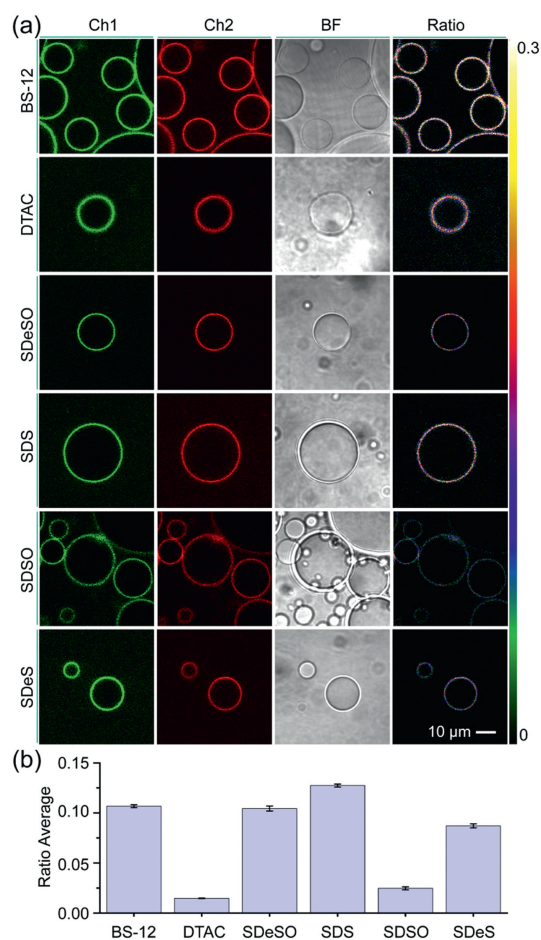


Fig. 4. (a) Confocal ratiometric imaging of artificial vesicles made from different surfactants labeled with **o-DAP**. The surfactants: BS-12, DTAC, SDeSO, SDS, SDeSO, SDeS. (b) The average ratio of artificial vesicles in (a). Data are presented as mean \pm standard deviation (SD) ($n=3$). Ex: 405 nm; collected: 420–490 nm in channel 1 and 490–590 nm in channel 2; Ratio: Ch2/Ch1. [**o-DAP**] = 10 $\mu\text{mol/L}$. [surfactants] = 3 mmol/L. Scale bar: 10 μm .

of the **o-DAP** sensor with various surfactants (Fig. 4b). This further proved the feasibility of the **o-DAP** sensor based on AEPF.

In summary, we have developed a sensor based on the AEPF, which successfully distinguished between cationic, anionic, zwitterionic, and nonionic surfactants, especially those with similar structures in the same type. The sensor based on AEPF was at-

Table 1
CMC values of surfactants.

Surfactant	CMC (mmol/L)		
	I_{445}/I_{560}	Literature reported	Ref.
CTAB	0.57	0.5	[32]
DTAB	12.59	14.6–16.0	[2]
DTAC	15.07	16.7	[33]
DDAC	1.45	1.2	[34]
SDS	8.43	8.0–8.2	[2]
SDeSO	39.92	0.024 mol/kg	[35]
SDBS	1.29	1.4–1.6	[2]
SDeSO	6.32	10.752	[36]
SDeS	33.63	35	[35]
SDC	4.05	3.92	[37]
BS-12	1.95	1.4–2.0	[2]
SB3-12	2.02	2–4	[38]
Triton X-100	0.45	0.24–0.27	[2]
NP40	1.09	0.673	[39]
Brij35	0.093	0.06	[40]
Tween20	0.015	0.011	[41]

tributed to the interaction between surfactants and **o-DAP**. The determination of CMC values for 16 surfactants and the discrimination of vesicles made from different surfactants further proved the feasibility of the AEPF-based sensor in recognizing various analytes.

Declaration of competing interest

The authors declare that they have no known competing financial interests or personal relationships that could have appeared to influence the work reported in this paper.

CRediT authorship contribution statement

Guangying Wang: Writing – original draft, Data curation. **Qinglong Qiao:** Writing – original draft, Supervision. **Wenhao Jia:** Conceptualization. **Yiyan Ruan:** Conceptualization. **Kai An:** Conceptualization. **Wenchao Jiang:** Conceptualization. **Xuelian Zhou:** Conceptualization. **Zhaochao Xu:** Writing – original draft, Supervision.

Acknowledgments

This work is supported by the National Natural Science Foundation of China (Nos. 22225806, 22078314, 22278394, 22378385) and Dalian Institute of Chemical Physics (Nos. DICPI202142, DICPI202436).

Supplementary materials

Supplementary material associated with this article can be found, in the online version, at doi:10.1016/j.ccllet.2024.110130.

References

- [1] X. Chen, S. Kang, M.J. Kim, et al., *Angew. Chem. Int. Ed.* 49 (2010) 1422–1425.
- [2] F. Deng, S. Long, Q. Qiao, Z. Xu, *Chem. Commun.* 54 (2018) 6157–6160.
- [3] Á.S. Inácio, K.A. Mesquita, M. Baptista, et al., *PLoS One* 6 (2011) e19850.
- [4] M.J.L. Castro, C. Ojeda, A.F. Cirelli, *Environ. Chem. Lett.* 12 (2014) 85–95.
- [5] R. Patel, K.S. Patel, *Analyst* 123 (1998) 1691–1695.
- [6] W.H. Chan, A.W.M. Lee, J.Z. Lu, *Anal. Chim. Acta* 361 (1998) 55–61.
- [7] J.M. Muriel, J.M. Bruque, J.M. Olias, et al., *Biotechnol. Lett.* 18 (1996) 235–240.
- [8] G. Könnecker, J. Regelmann, S. Belanger, K. Gamon, R. Sedlak, *Ecotox. Environ. Safe.* 74 (2011) 1445–1460.
- [9] G. Chang, Q. Zhang, L. Zhang, Y. Lü, T. Gao, *Environ. Prog. Sustain.* 34 (2015) 1142–1147.
- [10] J. Hrenovic, T. Ivankovic, *Open Life Sci.* 2 (2007) 405–414.
- [11] M. Wu, H. Xu, Y. Shen, W. Qiu, M. Yang, *Environ. Toxicol. Chem.* 30 (2011) 2335–2341.
- [12] S. Hussain, A.H. Malik, P.K. Iyer, *ACS Appl. Mater. Interfaces* 7 (2015) 3189–3198.
- [13] C.I. Tsoutsouvas, R.N. Kulkarni, A. Makriyannis, S.P. Nikas, *Expert Opin. Drug Dis.* 13 (2018) 933–947.
- [14] W. Liu, J. Chen, Q. Qiao, X. Liu, Z. Xu, *Chin. Chem. Lett.* 33 (2022) 4943–4947.
- [15] Y. Zhang, W. Zhou, N. Xu, et al., *Chin. Chem. Lett.* 34 (2023) 107472.
- [16] J. Li, Q. Qiao, Y. Ruan, et al., *Chin. Chem. Lett.* 34 (2023) 108266.
- [17] Y. Fan, Z. Liu, J. Wang, C. Cui, L. Hu, *Microchim. Acta* 190 (2023) 11.
- [18] H. Lin, Z. Xu, *Chin. Chem. Lett.* 33 (2022) 573–574.
- [19] J. Chen, W. Liu, X. Fang, Q. Qiao, Z. Xu, *Chin. Chem. Lett.* 33 (2022) 5042–5046.
- [20] J. Pan, W. Lin, F. Bao, Q. Qiao, G. Zhang, Y. Lu, Z. Xu, *Chin. Chem. Lett.* 34 (2023) 107519.
- [21] J.S. Lee, Y.K. Kim, M. Vendrell, Y.T. Chang, *Mol. Biosyst.* 5 (2009) 411–421.
- [22] M. Qiao, J. Fan, L. Ding, Y. Fang, *ACS Appl. Mater. Interfaces* 13 (2021) 18395–18412.
- [23] S. Rochat, J. Gao, X. Qian, F. Zaubitzer, K. Severin, *Chem. Eur. J.* 16 (2010) 104–113.
- [24] Z. Sun, Y.Z. Fan, S.Z. Du, et al., *Anal. Chem.* 92 (2020) 7273–7281.
- [25] D. Wei, H. Zhang, Y. Tao, et al., *Anal. Chem.* 96 (2024) 4987–4996.
- [26] M. Chhatwal, A. Kumar, V. Singh, R.D. Gupta, S.K. Awasthi, *Coord. Chem. Rev.* 292 (2015) 30–55.
- [27] S. Sandhu, R. Kumar, N. Tripathi, et al., *Sensor Actuat. B: Chem.* 241 (2017) 8–18.
- [28] Y. Huang, Y. Shen, S. Li, et al., *Sensors Actuat. B: Chem.* 348 (2021) 130679.
- [29] D. Tchoň, D. Bowskill, I. Sugden, P. Piotrowski, A. Makal, *J. Mater. Chem. C* 9 (2021) 2491–2503.
- [30] G.J. Yu, X.Y. Chen, S.Z. Mao, M.L. Liu, Y.R. Du, *Chin. Chem. Lett.* 28 (2017) 1413–1416.
- [31] A. Mohr, P. Talbiersky, H.G. Korth, et al., *J. Phys. Chem. B* 111 (2007) 12985–12992.
- [32] M.N. Fineman, J.W. McBain, *J. Phys. Chem.* 52 (1948) 881–896.
- [33] A. Jusufi, A.P. Hynninen, M. Haataja, A.Z. Panagiotopoulos, *J. Phys. Chem. B* 113 (2009) 6314–6320.
- [34] G. Rauwel, L. Leclercq, J. Criquelion, J.M. Aubry, V. Nardello-Rataj, *J. Colloid Interf. Sci.* 374 (2012) 176–186.
- [35] P. Roscigno, G. D'Errico, O. Ortona, R. Sartorio, L. Paduano, *Progr. Colloid Polym. Sci.* 122 (2003) 113–121.
- [36] R. Sadeghi, S. Shahabi, *J. Chem. Thermodyn.* 43 (2011) 1361–1370.
- [37] H. Wang, R. Dong, Z. Yang, et al., *Colloid. Surface. A* 436 (2013) 846–853.
- [38] G.A. Valbuena, L.V. Rao, J.R. Petersen, et al., *J. Chromatogr. A* 781 (1997) 467–474.
- [39] S. Dai, K.C. Tam, *Colloid. Surface. A* 229 (2003) 157–168.
- [40] S.K. Hait, S.P. Moulik, *J. Surfactants Deterg.* 4 (2001) 303–309.
- [41] A. Patit, S.S. Bhagwat, K.W. Penfield, P. Aikens, D.O. Shah, *J. Surfactants Deterg.* 3 (2000) 53–58.